13

Study of electrical resistance of gallium films on reconstructed Si(111) surface

© D.A. Tsukanov,[1,2] M.V. Ryzhkova[1]

[1] Institute of Automation and Control Processes, Far East Branch, Russian Academy of Sciences,
690041 Vladivostok, Russia
[2] Far Eastern Federal University, ,
690090 Vladivostok, Russia
e-mail: tsukanov@iacp.dvo.ru

Received April 25, 2024
Revised April 25, 2024
Accepted April 25, 2024

The results of a study of the crystal structure and electrical resistance of Si(111) silicon substrates after gallium deposition onto preformed surface reconstructions in the Ga/Si(111), Tl/Si(111), Au/Si(111) systems are presented. The work used the low-energy electron diffraction method to study changes in the structure of the surface crystal lattice, as well as a four-point probe method to measure the electrical resistance of substrates under in situ conditions. The influence of the concentration of adsorbed gallium atoms on the structural and electrical properties of films is considered. The role of surface reconstructions as a buffer layer for the subsequent growth of ultrathin films is demonstrated.

Keywords: adsorption, surface reconstruction, surface conductivity, low-energy electron diffraction, four-point probe method for measuring substrate resistance.

DOI: 10.61011/TP.2024.08.59001.143-24

Introduction

Ultrathin metal films and materials based on them attract close attention due to the increased interest in low-dimensional structures that can be used as instrument elements in micro- and nanoelectronics. Reduced electrical conductivity compared to bulk films made of the same material is one of the problems of such films. This is mainly attributable to the fact that the thickness of ultrathin films significantly limits the free path of electrons, however, the quality of epitaxial growth also plays an essential role, since defects in the crystal structure of films that occur during their growth greatly reduce the mobility of charge carriers, and, according to the Matthiessen's rule [1], they add their contribution to the increase of the electrical resistivity of the samples.

It is necessary to control the conditions of film growth for obtaining films with high structural quality, including the condition of the substrate surface on which the film is formed. The surface state in the ultrahigh vacuum conditions can be determined by the surface reconstruction of the substrate caused by modification of the uppermost layer of the crystal with respect to the structure of the corresponding atomic planes in the volume [2]. On the one hand, the reconstructions on the surface of Si(111) induced by the adsorption of metal atoms attract attention because of the wide variety of their structural and electronic properties [3–9]. On the other hand, the reconstructed surface itself can serve as a template for growing low-dimensional structures with unique properties [10–12], which can be used in nanoelectronics, optoelectronics and other applied fields where nanomaterials are in demand.

Recently, interest in ultrathin films and two-dimensional systems has continued to increase. Ultrathin gallium films constituting a two-dimensional metal can be attributed to such system among numerous similar studied systems and they also exhibit superconductivity properties on GaN(0001) substrates [13] and SiC [14]. In addition, gallium films exhibit a wide variety of structures depending on film thickness, substrate temperature and pressure, being the so-called „molecular" metal [15]. In this regard, the study of the conditions for the formation of ultrathin gallium films on the surface of silicon substrates may be of not only scientific but also practical interest.

One of the conditions for the formation of two-dimensional ultrathin gallium films on the surface of the Si(111) substrate is that gallium should be deposited on the surface with a preformed reconstruction, owing to which the adsorbed atoms will not interact with both the atoms of the silicon substrate and the atoms in the surface reconstruction. For example, lead atoms [16] or thallium can serve as such candidates. Thus, gallium and thallium slightly dissolve in each other and do not form bulk alloys, and when trying to form a joint alloy in such a film, their separate crystals are formed. Even in a liquid solution of these metals at a temperature of 500°C, an emulsion like water and oil appears [17]. Thus, it can be assumed that the mentioned properties of the Ga–Tl system will allow the formation of two-dimensional metal gallium films on the surface of the Si(111) substrate. In this system, an ordered thallium layer forms a buffer layer that will stabilize the first gallium layer

and suppress the formation of Ga/Si(111) reconstruction, in the case of which a predominantly defective film growth begins on the substrate [18].

In this paper, experimental studies of the formation conditions, periodic structure and electrical properties of ultrathin gallium films deposited on the surface of Si(111) with pre-prepared reconstructions of $\sqrt{3} \times \sqrt{3}$-Ga, 1×1-Tl, 6×6-Tl, $\sqrt{3} \times \sqrt{3}$-Au and others. The low-energy electron diffraction (LEED) method was used to control the crystal structure of the surface. Since it is well known that conductivity significantly depends on changes in the surface atomic structure and surface morphology (see, for example, [19–23]), the resistivity of Ga films grown on reconstructed Si(111) surfaces was measured using the four-probe method *in situ*, in order to determine how the conductive properties of such films can be improved depending on the concentration of the adsorbed material, their crystal structure and the surface structure of the initial substrate.

1. Experimental conditions

Ultrahigh vacuum chamber RIBER DEL-300 with an operating pressure of $\sim 10^{-10}$ Torr was used in this study. The unit is provided with low-energy electron diffractometer SPECTALEED from Scienta Omicron and a four-probe head for conducting electrical measurements under *in situ* conditions. The head is placed on a retractable manipulator, tungsten probes are located at the corners of a square with an inter-probe distance of 0.6 mm. Low-noise precision DC/AC current source Keithley 6221 and nanovoltmeter Keithley 2182A were used as meters, which in the delta system mode ensure a reliable and reproducible characterization of the materials under study by separating current and voltage measurements. Measurements of the electrical resistance of the samples were carried out under stable conditions in ultrahigh vacuum and at room temperature. The value of $R = U/I$ was used as the unit of measurement of electrical resistance, where I and U — the current values directly measured in the experiment (from 5 to 50 μA) and voltage, respectively, when passing direct current alternately through one pair of probes and measuring voltage on another pair with further averaging of the measurement results. The Si(111) substrate with an ultrathin metal film formed on the surface is a system of two parallel conduction channels (bulk substrate and film), therefore, all changes in the thin layer on the surface of the substrate (the amount of adsorbed material, the crystal structure of the film, its morphology, etc.) are recorded when measuring the resistivity of the substrate, which was used in the present work.

Rectangular silicon plates with the size of $15 \times 5 \times 0.45$ mm *n*-type, doped with phosphorus, with a resistivity of $300-1700\ \Omega\cdot$cm were used as samples. Sample surface was first cleaned by washing and cleaning in organic solvents with subsequent drying. Next, the samples were placed in an ultrahigh vacuum chamber, where they were first degassed at temperatures up to 600°C for several hours by alternating current, and then short-term heating (flash) was performed to a temperature of 1250°C. The samples prepared in this way showed a clear diffraction pattern 7×7, characteristic of the atomically pure silicon surface (see Appendix, Fig. 5, *a*).

Knudsen cells heated by direct current were used for sputtering of gallium and thallium. The gold was sputtered from a tungsten basket. The deposition rate of the adsorbed material was calibrated using LEED by diffraction patterns from the reconstructed surface with a known coverage value of the adsorbed material in monolayers (ML) (1 ML corresponds to the concentration of atoms $7.8 \cdot 10^{14}$ cm^{-2} for the non-reconstructed surface Si(111)). The error in the coverage of adsorbates calibrated in this way can be estimated as ± 0.05 ML. Before sputtering gallium on the substrate, surface reconstructions were preliminarily formed and the following were used as such reconstructions: Si(111)$\sqrt{3} \times \sqrt{3}$-Ga (see Appendix, fig. 5, *b*), Si(111)1×1-Tl (see Appendix, fig. 6, *a*), Si(111)6×6-Tl (see Appendix, fig. 7, *a*), Si(111)α-$\sqrt{3} \times \sqrt{3}$-Au (see Appendix, fig. 8, *a*) and Si(111)6×6-Au (see Appendix, Fig. 8, *d*). Surface reconstruction of Si(111)$\sqrt{3} \times \sqrt{3}$-Ga was formed by sputtering 0.3 ML of gallium onto a Si(111)7×7 substrate at a temperature of 450°C. Surface reconstruction of Si(111)1×1-Tl was obtained by sputtering 1 ML of thallium onto a Si(111)7×7 substrate at a temperature of 150−200°C. Surface reconstruction of Si(111)6×6-Tl was obtained by sputtering 1.4 ML of thallium onto the surface of Si(111)1×1-Tl at room temperature. Surface reconstructions of Si(111)$\alpha - \sqrt{3} \times \sqrt{3}$-Au and Si(111)$6 \times 6$-Au were obtained by sputtering 1 and 1.25 ML of gold, respectively, onto the atomically pure surface of the Si(111)7×7 substrate at a temperature of 750°C. The sputtering of gallium atoms on preformed reconstructions on a Si(111) substrate cooled to room temperature was used for obtaining gallium films.

2. Experimental results and their discussion

It is known that the surface of atomically pure silicon Si(111)7×7 is poorly suited for growing atomically smooth metal films due to the presence of broken bonds, which contribute to high chemical activity of the surface, as a result of which the layered growth of films is difficult. For example, the sputtering of gold, silver, indium and other metals on such a surface at room temperature leads to the formation of disordered amorphous films with low electrical conductivity due to significant scattering of charge carriers on the highly defective surface [24,25]. After annealing of such films at elevated temperatures, ordered reconstructions with a coverage of the adsorbed material of the order of one or less monolayer are observed on the surface, while

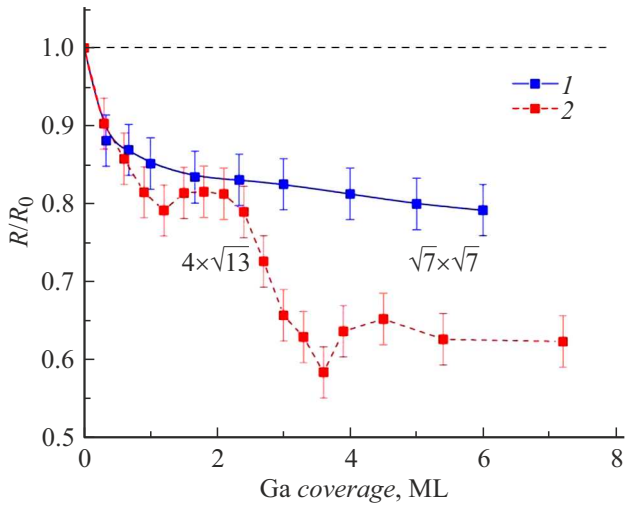

Figure 1. Electrical resistance of silicon samples after deposition of gallium on the surface of Si(111)7 × 7 (curve *1*) and the surface of Si(111)$\sqrt{3} \times \sqrt{3}$-Ga (curve *2*) at room temperature. The horizontal arrows show the areas of existence of surface reconstructions of Si(111)4 × $\sqrt{13}$-Ga and Si(111)$\sqrt{7} \times \sqrt{7}$-Ga according to the observed LEED patterns. The electrical resistance of an atomically pure Si(111) substrate is assumed to be R_0 7 × 7.

excess adsorbate atoms assemble into islands (growth by the Stranski–Krastanov mechanism).

Fig. 1 shows the behavior of the electrical resistance of the substrate after sputtering from 0 to 6 ML of gallium on the surface of atomically pure Si(111)7×7 at room temperature (curve *1*). Diffraction patterns show a gradual extinction of reflexes 7 × 7 with an increase of the gallium coverage, while no new reflexes are observed, which indicates the formation of an unordered gallium film. Annealing of such a substrate at a temperature of 450°C results in the appearance of a diffraction pattern $\sqrt{3} \times \sqrt{3}$, characteristic of the ordered reconstruction of gallium Si(111)$\sqrt{3} \times \sqrt{3}$-Ga [26], moreover, the electrical resistance of the substrate with this reconstruction differs slightly from the resistance of the original atomically pure Si(111) 7 × 7 substrate because both surfaces have low electrical conductivity. It should be noted that there are several more reconstructions in the Ga/Si(111) submonolayer system: Si(111)6.3 × 6.3-Ga, Si(111)11 × 11-Ga and Si(111)6.3$\sqrt{3} \times 6.3\sqrt{3}$-Ga, which are formed after annealing of the substrate at 560–600°C with gallium coverages of 0.6, 0.8 and 1 ML, respectively [3].

The following table shows the resistance values of the substrate measured on the same sample with reconstructions of Ga/Si(111). The sample was not subjected to high-temperature annealing, and the ordered phases were formed by adding an additional amount of gallium followed by annealing no higher than 550°C. The electrical resistance of the substrate was measured after a prolonged, more than 1 h, cooling of the substrate to room temperature. It can be seen that the resistance of a substrate with an unordered gallium film is about the same order as the resistance of a substrate with Si(111) 6.3$\sqrt{3} \times 6.3\sqrt{3}$-Ga reconstruction.

As noted in [27], for the growth of ordered gallium films, it is necessary to use a surface with a pre-prepared Si(111)$\sqrt{3} \times \sqrt{3}$-Ga reconstruction for avoiding the interaction of silicon atoms of the substrate with incoming gallium atoms during their adsorption. The fact is that the surface reconstructions of Si(111)6.3 × 6.3-Ga, Si(111)11 × 11-Ga and Si(111)6.3$\sqrt{3} \times 6.3\sqrt{3}$-Ga is a stressed (disproportionate) crystalline layer that contains a large number of defects due to the difference in the permanent lattices of silicon and gallium. Thus, the pre-prepared reconstruction of Si(111)$\sqrt{3} \times \sqrt{3}$-Ga on the surface of the sample will be a protective barrier separating the grown gallium film from the Si(111) substrate. Following this procedure, it was found from the LEED patterns that after sputtering approximately 1.5 ML of gallium onto the surface of Si(111)$\sqrt{3} \times \sqrt{3}$-Ga at room temperature, the surface structure of 4 × $\sqrt{13}$ is observed (see Appendix, Fig. 5, *c*), which, according to data obtained by scanning tunneling microscopy, corresponds to the formation of the first solid gallium layer [28]. Further sputtering of 2 ML of gallium results in the appearance of a diffraction pattern $\sqrt{7} \times \sqrt{7}$ (see Appendix, Fig. 5, *d*), which corresponds to the formation of the next gallium layer completely covering the entire surface of the substrate. Moreover, it is reported in the paper [28] that this ordered gallium layer is described as the crystal structure of gallenine, a two-dimensional gallium layer on the surface of the film.

Electrical measurements showed that the sputtering of gallium on Si(111)$\sqrt{3} \times \sqrt{3}$-Ga surface at room temperature reduces the resistance of the substrate. Figure 1 shows the results of measurements of the electrical resistance of the substrate by the four-probe method, depending on the amount of adsorbed gallium, with LEED control of the state of the crystal structure of the surface (curve *2*). It can be seen that when a coverage corresponding to the area of existence of the surface reconstruction 4 × $\sqrt{13}$ is reached, the resistance reaches a plateau, and then decreases until a new surface reconstruction $\sqrt{7} \times \sqrt{7}$ is formed on the surface, and after that the electrical resistance of the substrate remains at about the same level. This behavior is very similar to the oscillations of electrical resistance that occur during the layered growth of a metal film [29]. In the case of a gallium film, it can be noted that an increase of resistance is observed with gallium coverages corresponding to the initial stage of formation of surface phases of both 4 × $\sqrt{13}$ and $\sqrt{7} \times \sqrt{7}$, when diffraction patterns are already recorded using LEED, but the surface represents extensive areas of surface reconstruction [27], which are separated from each other and do not form a percolation path for electric current; thus, conditions are created for the scattering of charge carriers at numerous domain boundaries and inhomogeneities. As soon as such a phase coalesces on the entire surface of the substrate, the percolation threshold is overcome, and the conductivity of

The value of the electrical resistance of the Si(111) substrate for samples with surface reconstructions

Sample surface	Electric resistance R, Ω	Relationship R/R_0
Si(111) 7×7	1394 ± 64	1
Si(111)$\sqrt{3} \times \sqrt{3}$-Ga	1308 ± 14	0.94
Si(111)6.3×6.3-Ga	1107 ± 30	0.79
Si(111)$6.3\sqrt{3} \times 6.3\sqrt{3}$-Ga	1024 ± 22	0.73
Si(111)$4 \times \sqrt{13}$-Ga	1172 ± 9	0.84
Si(111)$\sqrt{7} \times \sqrt{7}$-Ga	916 ± 30	0.66
Si(111)α-$\sqrt{3} \times \sqrt{3}$-Au	930 ± 30	0.67
Si(111)$3\sqrt{3} \times 3\sqrt{3}$-(Au,Ga)	508 ± 15	0.36
Si(111)2×2-(Au,Ga)	383 ± 6	0.27

Note. R_0 — electrical resistance of a sample with an atomically pure surface Si(111)7×7.

the film begins to increase (accordingly, the resistance on the graph decreases).

The proposed model of the atomic structure in Ref. [27] represents a system of several layers of gallium atoms: the first layer of gallium atoms (1 ML) is directly adjacent to the non-reconstructed surface Si(111), there is an overlying double layer of gallium atoms (the gallium coverage is estimated as 2.14 ML), the remaining gallium atoms on top of these layers are in the state of adatoms that are sufficiently mobile on the surface, and an increase in their concentration does not change the diffraction pattern $\sqrt{7} \times \sqrt{7}$. The model of atomic structure and reconstruction $4 \times \sqrt{13}$ [28] looks similar, when the surface does not rebuild into $\sqrt{7} \times \sqrt{7}$ for some time after increase of the gallium coverage, until the gallium atoms reach the desired concentration on the surface. This also explains the plateau on the resistance graph, since adatoms do not form a continuous layer or agglomerations, respectively, they do not participate in the formation of a conductive layer. As for the studies of the electronic structure for this system, the electronic states were measured in Ref. [27] using photoelectron spectroscopy with angular resolution, which showed that there are metallic filled states in the band gap that are strongly blurred near the Fermi level, which speaks in favor of the presence of Anderson localization caused by weak disorder of the system. Thus, the formation of the Si(111)$\sqrt{3} \times \sqrt{3}$-Ga buffer layer promotes the growth of a smooth ultrathin gallium film on the substrate surface, however, the presence of a weak disorder caused by layer tension limits the conductive properties of this material. At the same time, the conductivity of the surface phase of Si(111)$\sqrt{7} \times \sqrt{7}$-Ga turns out to be higher because of a higher concentration of metal atoms than for the surface phases of Si(111)6.3×6.3-Ga, Si(111)$6.3\sqrt{3} \times 6.3\sqrt{3}$-Ga and Si(111)$4 \times \sqrt{13}$-Ga (see table).

Reconstructions in the Tl/Si(111) system were chosen as another buffer layer for the growth of ultrathin gallium films. For example, the reconstruction of Si(111)1×1-Tl is a single layer of thallium atoms located at T_4 sites on a volume-like lattice of silicon Si(111) with 1 ML of thallium atom coverage [30]. Thus, the interaction of gallium atoms with silicon atoms of the substrate is excluded; moreover, as mentioned above, gallium atoms and thallium atoms interact weakly with each other and do not form joint compounds or alloys. A reconstruction of Si(111)6×6-Tl was used as another surface in the experiment, which is a double layer of thallium atoms with a common 2.4 ML coverage providing a diffraction pattern of „6×6“ [31].

Gallium was sprayed at room temperature onto a Si(111) substrate with pre-prepared reconstructions induced by thallium adsorption. It was found using low-energy electron diffraction that the substrate surface rearranges its crystal structure with an increase of the coverage of adsorbed gallium at room temperature. Thus, deposition of 1 ML of gallium on the reconstruction of Si(111)1×1-Tl leads first to the formation of reconstruction of 5×5 (see Appendix, Fig. 6, *b*), and then 5×1; further sputtering from 1 to 1.2 ML of gallium results in a formation of diffraction pattern 9×9 (see Appendix, fig. 6, *c*); then the pattern 7×3 is observed (see Appendix, fig. 6, *d*), formed after sputtering of about 1.2−1.3 ML of gallium, and the following pattern 5×5 (see Appendix, Fig. 6, *e*) is visible after sputtering from 1.3 to 2 ML of gallium. The sputtering of gallium in the coverage range from 0 to 2.5 ML on the reconstruction of Si(111)6×6-Tl causes the sequential formation of reconstructions „9×9“ (see Appendix, Fig. 7, *b*), 5×1 (see Appendix, fig. 7, *c*), „4×3“ (see Appendix, Fig. 7, *d*) and $\sqrt{7} \times \sqrt{7}$ (see Appendix, Fig. 7, *e*) (the designation of the lattice translation vectors in quotation marks here means that the diffraction patterns are a reflection of a disproportionate lattice, which can also be caused by the tension of the surface layer). Based on the fact that these diffraction patterns have never been observed separately before either for the submonolayer Tl/Si(111) system or for the Ga/Si(111) system, it can be said that the reconstructions obtained in the experiment are the result of the formation of an ordered film, the crystal structure of which includes both gallium atoms and thallium atoms, the exact location of which can be determined by comparing the data of scanning tunneling microscopy and calculations of

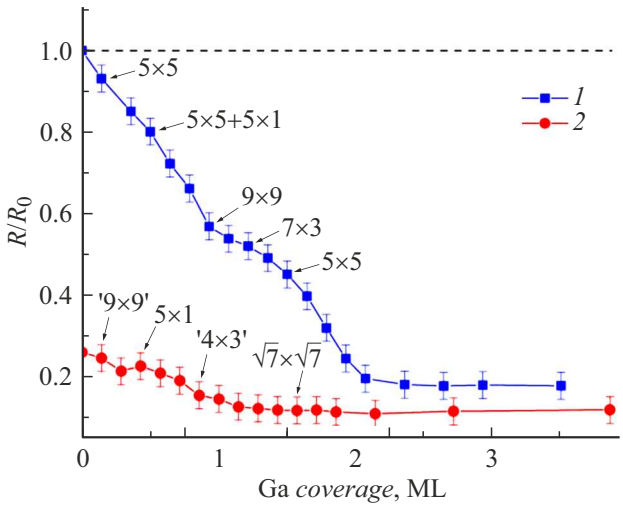

Figure 2. Electrical resistance of silicon samples after gallium deposition on the surface with reconstruction of Si(111)1 × 1-Tl (curve *1*) and reconstruction of Si(111)6 × 6-Tl (curve *2*) at room temperature. The arrows indicate the points at which the corresponding diffraction patterns were observed.

the crystal structure from the first principles. In addition, it was found that these structures are preserved on the surface up to the substrate temperature 150–200°C.

Figure 2 shows the results of measurements of the electrical resistance of the Si(111) substrate after deposition of gallium on the reconstructed surface 1 × 1-Tl (curve *1*), as well as on the surface with another reconstruction of thallium — Si(111)6 × 6-Tl (curve *2*). It can be seen that the initial surfaces have different properties: for example, a substrate with an ordered thallium layer 1 × 1-Tl has a high resistance, approximately corresponding to the electrical resistance of an atomically pure silicon substrate Si(111)7 × 7, while the substrate with reconstruction Si(111)6 × 6-Tl demonstrates low resistance, since it is well known that this phase is a two-dimensional metal [32]. However, in both cases, the sputtering of gallium on these surfaces results in a decrease of resistance, which reaches saturation after deposition of over 2.5 ML of gallium. What is significant in these results is that the decrease of resistance R is not monotonous, in accordance with the ratio $R \propto 1/d$, characteristic of metal films depending on their thickness, where d — film thickness [33], but it has an almost stepwise pattern, as can be seen in Fig. 2 (curve *1*), for example, in case of transition from the structure 5 × 1 to 9 × 9, from 9 × 9 to 7 × 3 and so on. It can be seen from the graph that, firstly, such changes of resistance correlate well with the restructuring of the surface structure, when the less dense surface phase changes to a denser phase that exists in a certain range of concentrations of adsorbed atoms, and secondly, a gradual decrease of resistance may be a sign of layered film growth due to an increase in concentration metal atoms on the surface. An approximate film thickness of 3–4 atomic layers can be estimated based on the concentration of metal atoms estimated from the coverage values obtained during calibration of the sources of the adsorbed material (gallium and thallium). Further, the output of the dependence of the resistance on the concentration of gallium on saturation indicates that the further growth of the film (after coverage with more than 2.5 ML of gallium more) takes place according to the island mechanism. Another feature is that surfaces with different initial thallium reconstruction, Si(111)1 × 1-Tl or Si(111)6 × 6-Tl, but with the same crystal structure of the surface according to diffraction data, for example, Si(111)5 × 1-(Tl,Ga) have different electrical resistance, which may be attributable to different concentrations of thallium atoms in them, corresponding to 1 and 2.4 ML coverage, respectively. This means that the surface lattice is displayed in the same way from the point of view of the LEED, but the concentration of atoms in the structural layers of the film may be different, which requires additional studies. Moreover, in all cases, it is obvious that the deposition of gallium reduces the electrical resistance of the system, which also has a structural ordering, which, for example, allows controlling the thickness of such a film with very high accuracy, and, knowing the dependence of resistance on thickness, calculating its electrical parameters by observing the crystal structure of its surface.

(Ga,Au)/Si(111) system was used as an example of a film in which the adsorbed elements interact with each other to form an alloy. It is known [34] that the sputtering of gallium on the surface of Si(111)α-$\sqrt{3}\times\sqrt{3}$-Au at room temperature results in the formation of islands of alloy $AuGa_2$ on the surface of the substrate. At the first stage of adsorption (gallium coverage $1 \leq$ ML), gallium covers the initial surface in such a way that gallium atoms on the surface $\sqrt{3}\times\sqrt{3}$ form an unordered top layer. Islands of alloy $AuGa_2$ begin to form on the surface with further sputtering of gallium (over 1 ML), and gold atoms are extracted from the lower layer in the alloying process, and active mixing of gold and gallium atoms begins [34]. These results are confirmed in this paper by observations of diffraction patterns: the reflexes of the initial structure $\sqrt{3}\times\sqrt{3}$ begin to fade and disappear completely after sputtering of about 2 ML of gallium, and the main reflexes from the silicon lattice of Si(111)1 × 1 become weak. Electrical measurements for this substrate showed (Fig. 3, curve *1*) that at the first stage the resistance increases due to the destruction of the surface reconstruction of gold, and at the second stage the resistance changes are already insignificant, since islands are forming on top of a double layer of gallium and gold atoms alloy. The resistance of the substrate with another reconstruction of gold Si(111)6 × 6-Au behaves similarly after gallium sputtering: with an increase of the amount of adsorbed gallium, an increase in the electrical resistance of the substrate is first observed, then its saturation occurs (Fig. 3, curve *2*). The difference from the curve *1* consists in the fact that the saturation of the resistance occurs a little later (with a larger gallium coverage), and also the resistance of

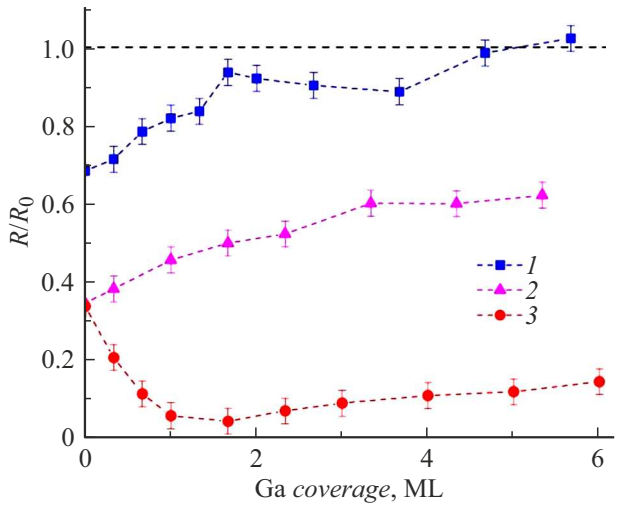

Figure 3. Electrical resistance of silicon samples after gallium deposition at room temperature on the surface with reconstruction of Si(111)α-$\sqrt{3} \times \sqrt{3}$-Au (curve *1*), reconstruction of Si(111)6×6-Au (curve *2*) and atomically pure substrate of Si(111)7×7 with a preformed amorphous gold layer (~ 1 ML of Au) (curve *3*).

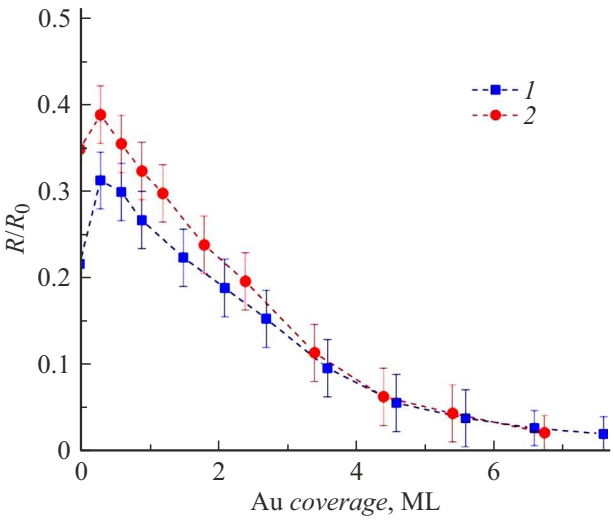

Figure 4. Electrical resistance of silicon samples after gold deposition at room temperature on the substrate surface with reconstruction Si(111)2×2-(Au,Ga) (curve *1*) and reconstruction Si(111)$3\sqrt{3} \times 3\sqrt{3}$-(Au,Ga) (curve *2*).

the substrate at the final stage of measurements remains lower than in the previous case. This is attributable to the fact that the gold coverage on the original surface (surface reconstruction Si(111)6×6-Au) is higher than for the surface Si(111)α-$\sqrt{3} \times \sqrt{3}$-Au (1.25 and 1 ML, respectively [35]), which means that the formation of a solid layer of alloy with stoichiometry $AuGa_2$ shifts along the gallium coverage towards a higher concentration, which significantly affects the conductive properties for these surfaces. The resistance behavior of the disordered gold film after gallium sputtering is of interest from this point of view (Fig. 3, curve *3*). The fact is that the sputtering of 1 ML of gold at room temperature on the surface of the substrate Si(111)7×7 results in the formation of an amorphous film in which conductivity occurs through percolation [22], since areas with remnants of reconstruction 7×7 of pure silicon [36] remain on the surface, which is noted in diffraction patterns in the form of structure $\delta 7 \times 7$. The arriving gallium atoms fill the free areas of the surface due to interaction with silicon atoms and form a continuous film, respectively, its resistance decreases, and then the resistance increases, as the alloy formation process begins, which is accompanied by the extraction of gold atoms from the film to form islands of $AuGa_2$.

The formation of ordered reconstructions is an interesting feature of the (Au,Ga)/Si(111) system. It was found that well-ordered surface phases Si(111)$3\sqrt{3} \times 3\sqrt{3}$-(Au,Ga) are formed on the surface (see Appendix, Fig. 8, *b*) and Si(111)2×2-(Au,Ga), respectively, if 0.15 or 0.6 ML of gallium is sputtered on the surface of Si(111)α-$\sqrt{3} \times \sqrt{3}$-Au at the substrate temperature of 350°C (see Appendix, fig. 8, *c*). The substrate resistance values measured for these surfaces are shown in the table. It can be seen that, in contrast to the experiment with the sputtering of gallium on the surface of Si(111)α-$\sqrt{3} \times 3$-Au at room temperature the resistance of the substrate with Si(111)2×2-(Au,Ga) phase is lower with approximately the same amount of adsorbed gallium, which indicates that the conductivity of the ordered system is higher than conductivity of a film with the same stoichiometric composition, but with poor structural quality. On the other hand, the ordered reconstruction, as mentioned above, can serve as a buffer layer preventing the interaction of the adsorbed material with the atoms of the substrate.

In particular, Figure 4 shows the results of an experiment to measure the resistance of a substrate after sputtering of up to 7–8 ML of gold at room temperature on reconstructed surfaces of Si(111) $3\sqrt{3} \times 3\sqrt{3}$-(Au,Ga)(curve *1*) and Si(111)2×2-(Au,Ga) (curve *2*). Two features of resistance behavior can be noted. A slight increase of resistance is observed at the initial stage of gold sputtering. This may be attributable to two reasons: firstly, at this stage (up to 1 ML of gold), the system is disordered because of the incoming adsorbed atoms, when the room temperature of the substrate is insufficient for formation of a new surface phase, and secondly, a charge may change in the near-surface region of the substrate, which was previously assumed for the case of gold sputtering on the surface of Si(111)α-$\sqrt{3} \times \sqrt{3}$-Au [23]. In this case, it can be assumed that both of these factors are important. A rapid decrease of resistance due to the formation of a solid gold film on the surface is observed at the second stage (after sputtering of more than 1–1.5 ML of gold). This dependence of resistance on the amount of adsorbed gold suggests that we are dealing with a layered growth of an ultrafine gold film in this case. The monotonous nature of the graphs, as well as the lack of an ordered structure according to the LEED

data, indicate that the gold film grows uniformly without the formation of ordered reconstructions or an obvious island mechanism of film growth during growth.

Conclusion

As a result of experiments conducted for studying the effect of gallium adsorption on the crystal structure and electrical resistance of Si(111) silicon substrates with reconstructions formed on their surface, it was found that the electrical resistance of samples with ultrathin gallium films depends not only on the degree of coverage of the adsorbed material, but also correlates well with the crystal structure of the film, which, in turn, is determined by the way the atoms of the adsorbed gallium interact with the underlying surface reconstruction that in this case plays the role of a buffer layer preventing the interaction of gallium with the atoms of the substrate. The following surface reconstructions were used: Si(111)$\sqrt{3} \times \sqrt{3}$-Ga, Si(111)1×1-Tl, Si(111)6×6-Tl, Si(111)α-$\sqrt{3} \times \sqrt{3}$-Au and Si(111)6×6-Au. It was found that the lowest electrical resistance is demonstrated by gallium films deposited on the reconstructed surfaces of Si(111)1×1-Tl and Si(111)6×6-Tl.

Funding

The work was performed under the state assignment of the Ministry of Science and Higher Education of the Russian Federation (FWRM-2021-0002).

Conflict of interest

The authors declare that they have no conflict of interest.

Appendix

Low-energy electron diffraction patterns for the samples used in this study

Figure 5–8 shows diffraction patterns for surface reconstructions obtained in the study with an electron energy of 40 eV. Lattice cells of the surface of Si(111)1×1 substrate (dotted line) and translation vectors for lattice cells of surface reconstruction (arrows) are shown for reach reconstruction. The numbers indicate the numbers of the main reflexes of Si(111)1×1 substrate (only in Fig. 5, *a*), as well as the translation periods for superreflexes. Diffraction patterns for more complex superstructures such as Si(111)$4 \times 3 + 7 \times 3$-(Ga,Tl), Si(111) 7×3-(Ga,Tl) and Si(111)$4 \times \sqrt{13}$-Ga, shown in Fig. 9 together with the diagrams of the location of reflexes obtained using the LEEDPat program [37]. The symmetry of the crystal structure of the surface of the Si(111) substrate allows the existence of several symmetrically equivalent domains [38], usually three domains and six domains for lattice $4 \times \sqrt{13}$.

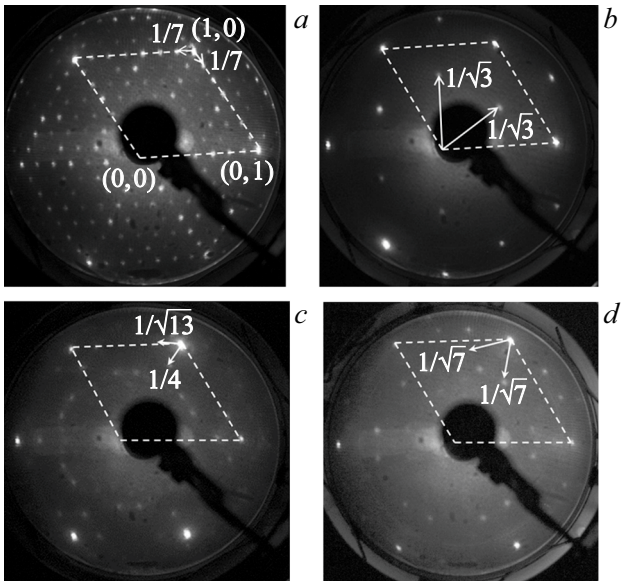

Figure 5. Low-energy electron diffraction patterns for surfaces: *a* — Si(111)7×7; *b* — Si(111)$\sqrt{3} \times \sqrt{3}$-Ga; *c* — Si(111)$4 \times \sqrt{13}$-Ga; *d* — Si(111)$\sqrt{7} \times \sqrt{7}$-Ga. Beam energy 40 eV.

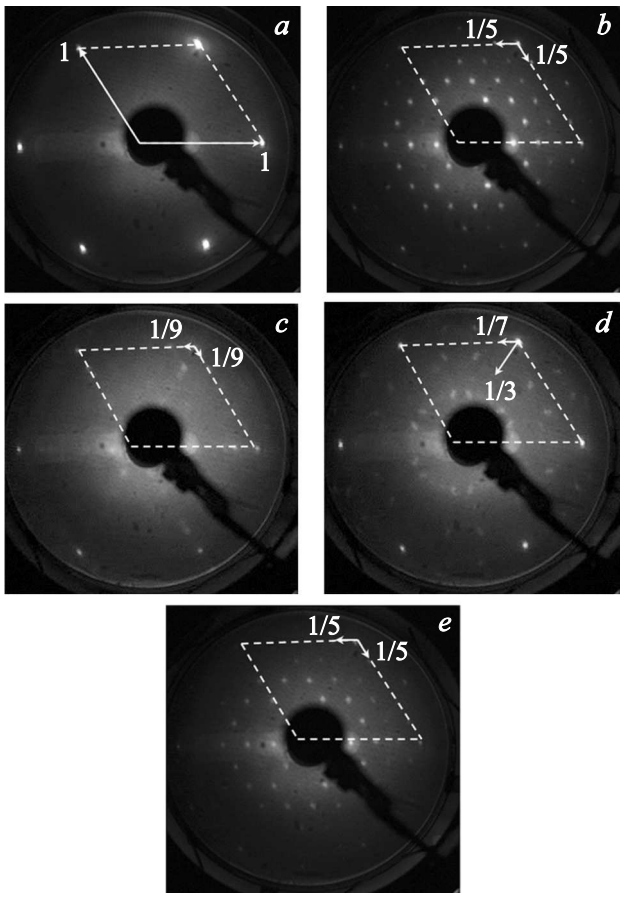

Figure 6. Low-energy electron diffraction patterns for surfaces :*a* — Si(111)1×1-Tl; *b* — Si(111)5×5-(Ga,Tl); *c* — Si(111)9×9-(Ga,Tl); *d* — Si(111)7×3-(Ga,Tl); *e* — Si(111)5×5-(Ga,Tl). Beam energy 40 eV.

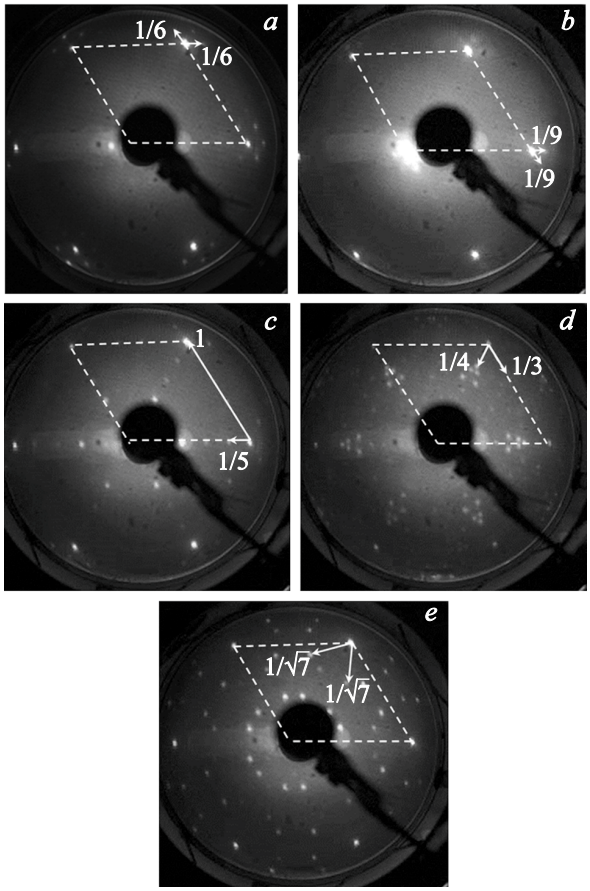

Figure 7. Low-energy electron diffraction patterns for surfaces: *a* — Si(111)6 × 6-Tl; *b* — Si(111)9 × 9-(Ga,Tl); *c* — Si(111)5 × 1-(Ga,Tl); *d* — Si(111)4 × 3 + 7 × 3-(Ga,Tl); *e* — Si(111)$\sqrt{7} \times \sqrt{7}$-(Ga,Tl). Beam energy 40 eV.

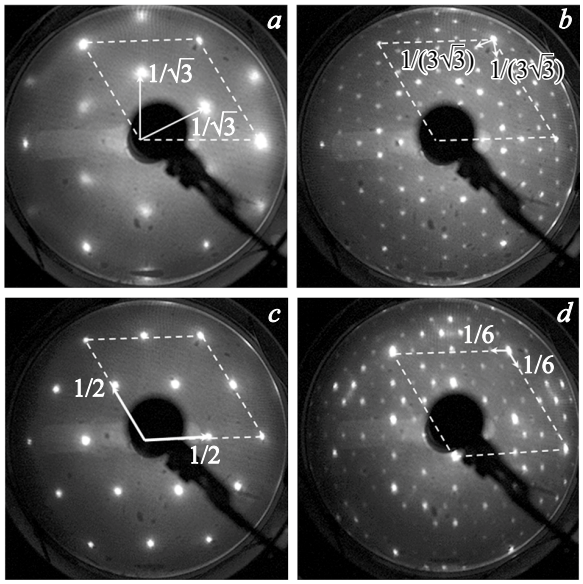

Figure 8. Low-energy electron diffraction patterns for surfaces: *a* — Si(111)α-$\sqrt{3} \times \sqrt{3}$-Au; *b* — Si(111)$3\sqrt{3} \times 3\sqrt{3}$-(Au,Ga); *c* — Si(111)2 × 2-(Au,Ga); *d* — Si(111)6 × 6-Au. Beam energy 40 eV.

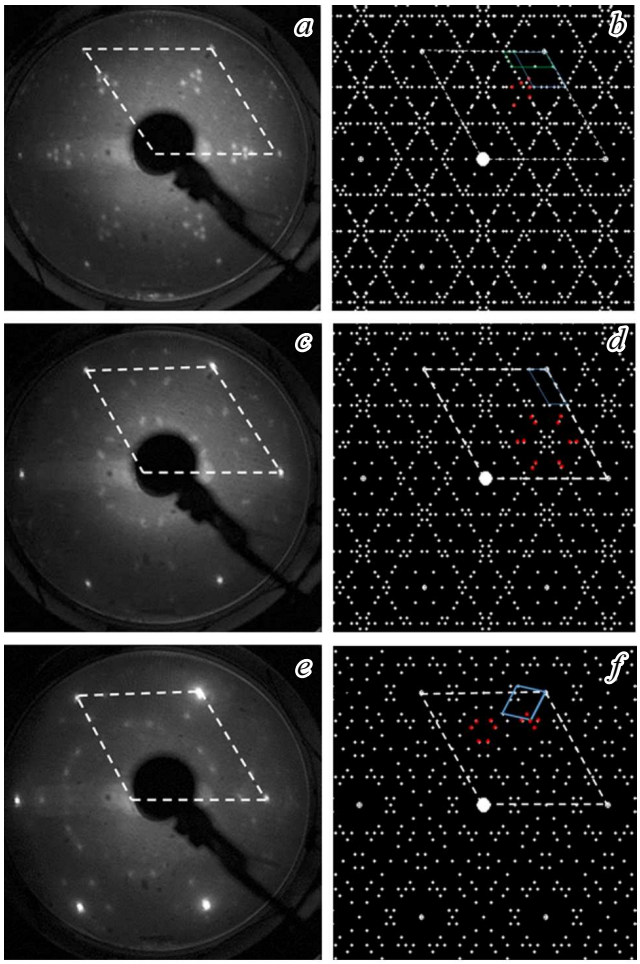

Figure 9. Low-energy electron diffraction patterns and their corresponding reflection patterns for the following surfaces: Si(111)4 × 3 + 7 × 3-(Ga,Tl) (*a, b*), Si(111)7 × 3-(Ga,Tl) (*c, d*), Si(111)4 × $\sqrt{13}$-Ga (*e, f*). The reflexes that are visible in the diffraction pattern are shown by red color in the diagram.

For clarity, the red color on the diagrams highlights the reflexes that are visible in the diffraction pattern and are characteristic of this particular periodic structure, since the remaining reflexes can only be detected at other energies of the primary beam.

References

[1] W.F. Leonard, S.F. Lin. Thin Solid Films, **28**, L9 (1975). DOI: 10.1016/0040-6090(75)90285-0
[2] C.B. Duke. Appl. Surf. Sci., **65/66**, 543 (1993). DOI: 10.1016/0169-4332(93)90717-P
[3] V.G. Lifshits, A.A. Saranin, A.V. Zotov. *Surface Phases on Silicon* (Chichester, Wiley, 1993)
[4] H.W. Yeom, S. Takeda, E. Rotenberg, I. Matsuda, K. Horikoshi, J. Schaefer, C.M. Lee, S.D. Kevan, T. Ohta, T. Nagao, S. Hasegawa. Phys. Rev. Lett., **82**, 4898 (1999). DOI: 10.1103/PhysRevLett.82.4898

[5] E. Rotenberg, H. Koh, K. Rossnagel, H.W. Yeom, J. Schäfer, B. Krenzer, M.P. Rocha, S.D. Kevan. Phys. Rev. Lett., **91**, 246404 (2003). DOI: 10.1103/PhysRevLett.91.246404
[6] K. Sakamoto, H. Kakuta, K. Sugawara, K. Miyamoto, A. Kimura, T. Kuzumaki, N. Ueno, E. Annese, J. Fujii, A. Kodama, T. Shishidou, H. Namatame, M. Taniguchi, T. Sato, T. Takahashi, T. Oguchi. Phys. Rev. Lett., **103**, 156801 (2009). DOI: 10.1103/PhysRevLett.103.156801
[7] T. Uchihashi, P. Mishra, M. Aono, T. Nakayama. Phys. Rev. Lett., **107**, 207001 (2011). DOI: 10.1103/PhysRevLett.107.207001
[8] Y. Fukuya, I. Matsuda, M. Hashimoto, K. Kubo, T. Hirahara, S. Yamazaki, W.H. Choi, H.W. Yeom, S. Hasegawa, A. Kawasuso, A. Ichimiya. Surf. Sci., **606**, 919 (2012). DOI: 10.1016/j.susc.2012.02.006
[9] I. Matsuda, F. Nakamura, K. Kubo, T. Hirahara, S. Yamazaki, W.H. Choi, H.W. Yeom, H. Narita, Y. Fukuya, M. Hashimoto, A. Kawasuso, M. Ono, Y. Hasegawa, S. Hasegawa, K. Kobayashi. Phys. Rev. B, **82**, 165330 (2010). DOI: 10.1103/PhysRevB.82.165330
[10] V.G. Kotlyar, A.V. Zotov, A.A. Saranin, T.V. Kasyanova, M.A. Cherevik, I.V. Pisarenko, V.G. Lifshits. Phys. Rev. B, **66**, 165401 (2002). DOI: 10.1103/PhysRevB.66.165401
[11] K. Oura, V.G. Lifshits, A.A. Saranin, A.V. Zotov, M. Katayama. Surf. Sci. Reps., **35**, 1 (1999). DOI: 10.1016/S0167-5729(99)00005-9
[12] D.A. Tsukanov, M.V. Ryzhkova, D.V. Gruznev, O.A. Utas, V.G. Kotlyar, A.V. Zotov, A.A. Saranin. Nanotechnology, **19**, 245608 (2008). DOI: 10.1088/0957-4484/19/24/245608
[13] H.-M. Zhang, Y. Sun, W. Li, J.-P. Peng, C.-L. Song, Y. Xing, Q. Zhang, J. Guan, Y. Zhao, S. Ji, L. Wang, K. He, X. Chen, L. Gu, L. Ling, M. Tian, L. Li, X.C. Xie, J. Liu, H. Yang, Q.-K. Xue, J. Wang, X. Ma. Phys. Rev. Lett., **114**, 107003 (2015). DOI: 10.1103/PhysRevLett.114.107003
[14] N. Briggs, B. Bersch, Y. Wang, J. Jiang, R.J. Koch, N. Nayir, K. Wang, M. Kolmer, W. Ko, A.D.L.F. Duran, S. Subramanian, C. Dong, S. Shallenberger, M. Fu, Q. Zou, Y.-W. Chuang, Z. Gai, A.-P. Li, A. Bostwick, C. Jozwiak, C.-Z. Chang, E. Rotenberg, J. Zhu, A.C.T. van Duin, V. Crespi, J.A. Robinson. Nat. Mater., **19**, 637 (2020). DOI: 10.1038/s41563-020-0631-x
[15] D.Z. Metin, L. Hammerschmidt, N. Gaston. Phys. Chem. Chem. Phys., **20**, 27668 (2018). DOI: 10.1039/c8cp05280h
[16] L.V. Bondarenko, A.Y. Tupchaya, Y.E. Vekovshinin, D.V. Gruznev, V.G. Kotlyar, T.V. Utas, A.N. Mihalyuk, N.V. Denisov, A.V. Zotov, A.A. Saranin. J. Alloys Compd., **969**, 172453 (2023). DOI: 10.1016/j.jallcom.2023.172453
[17] H. Okamoto, M.E. Schlesinger, E.M. Mueller. *ASM Handbook Volume 3: Alloy Phase Diagrams* (ASM International, 2016)
[18] M.Y. Lai, Y.L. Wang. Phys. Rev. B, **60**, 1764 (1999). DOI: 10.1103/PhysRevB.60.1764
[19] E.Z. Luo, S. Heun, M. Kennedy, J. Wollschlager, M. Henzler. Phys. Rev. B, **49**, 4858 (1994). DOI: 10.1103/PhysRevB.49.4858
[20] T. Kanagawa, R. Hobara, I. Matsuda, T. Tanikawa, A. Natori, S. Hasegawa. Phys. Rev. Lett., **91**, 036805 (2003). DOI: 10.1103/PhysRevLett.91.036805
[21] D.A. Tsukanov, S.G. Azatyan, M.V. Ryzhkova, E.A. Borisenko, O.A. Utas, A.V. Zotov, A.A. Saranin. Appl. Surf. Sci., **476**, 1 (2019). DOI: 10.1016/j.apsusc.2019.01.063
[22] D.V. Gruznev, D.A. Olyanich, D.N. Chubenko, D.A. Tsukanov, E.A. Borisenko, L.V. Bondarenko, M.V. Ivanchenko, A.V. Zotov, A.A. Saranin. Surf. Sci., **603**, 3400 (2009). DOI: 10.1016/j.susc.2009.10.001
[23] S. Hasegawa, X. Tong, S. Takeda, N. Sato, T. Nagao. Prog. Surf. Sci., **60**, 89 (1999). DOI: 10.1016/S0079-6816(99)00008-8
[24] O. Pfennigstorf, K. Lang, H.-L. Günter, M. Henzler. Appl. Surf. Sci., **162**, 537 (2000). DOI: 10.1016/S0169-4332(00)00247-6
[25] S. Hasegawa, S. Ino. Surf. Sci., **283**, 438 (1993). DOI: 10.1016/0039-6028(93)91016-I
[26] P. Kumar, M. Kumar, B.R. Mehta, S.M. Shivaprasad. Appl. Surf. Sci., **256**, 480 (2009). DOI: 10.1016/j.apsusc.2009.07.036
[27] L.V. Bondarenko, A.Y. Tupchaya, Y.E. Vekovshinin, D.V. Gruznev, A.N. Mihalyuk, D.V. Denisov, A.V. Matetskiy, D.A. Olyanich, T.V. Utas, V.S Zhdanov, A.V. Zotov, A.A. Saranin. Mol. Syst. Des. Eng., **8**, 604 (2023). DOI: 10.1039/d2me00251e
[28] M.L. Tao, Y.B. Tu, K. Sun, Y.L. Wang, Z.B. Xie, L. Liu, M.X. Shi, J.Z. Wang. 2D Mater., **5**, 035009 (2018). DOI: 10.1088/2053-1583/aaba3a
[29] M. Jalochowski, E. Bauer. Surf. Sci., **213**, 556 (1989). DOI: 10.1016/0039-6028(89)90312-9
[30] S.S. Lee, H.J. Song, N.D. Kim, J.W. Chung, K. Kong, D. Ahn, H. Yi, B.D. Yu, H. Tochihara. Phys. Rev. B, **66**, 233312 (2002). DOI: 10.1103/PhysRevB.66.233312
[31] A.N. Mihalyuk, L.V. Bondarenko, A.Y. Tupchaya, D.V. Gruznev, J.-P. Chou, C.-R. Hsing, C.-M. Wei, A.V. Zotov, A.A. Saranin. Surf. Sci., **668**, 17 (2018). DOI: 10.1016/j.susc.2017.10.010
[32] S. Ichinokura, L.V. Bondarenko, A.Y. Tupchaya, D.V. Gruznev, A.V. Zotov, A.A. Saranin, S. Hasegawa. 2D Mater., **4**, 025020 (2017). DOI: 10.1088/2053-1583/aa57f9
[33] Y. Ke, F. Zahid, V. Timoshevskii, R. Xia, D. Gall, H. Guo. Phys. Rev. B, **79**, 155406 (2009). DOI: 10.1103/PhysRevB.79.155406
[34] T. Yamanaka, S. Ino. Phys. Rev. Lett., **89**, 196101 (2002). DOI: 10.1103/PhysRevLett.89.196101
[35] L.V. Bondarenko, A.N. Mihalyuk, A.Y. Tupchaya, Y.E. Vekovshinin, D.V. Gruznev, A.V. Zotov, A.A. Saranin. Phys. Rev. B, **101**, 075405 (2020). DOI: 10.1103/PhysRevB.101.075405
[36] I. Chizhov, G. Lee, R.F. Willis. Phys. Rev. B, **56**, 12316 (1997). DOI: 10.1103/PhysRevB.56.12316
[37] *Fritz Haber Institute of the Max Planck Society, „LEEDpat4“ software* https://www.fhi.mpg.de/958975/LEEDpat4
[38] K. Oura, V.G. Lifshits, A.A. Saranin, A.V. Zotov, M. Katayama. *Vvedenie v fiziku poverkhnosti* (Nauka, M., 2006) (in Russian)

Translated by A.Akhtyamov